Heterogeneity of Biofilms in Rotating Annular Reactors: Occurrence, Structure, and Consequences

A. Gjaltema,[1]* P. A. M. Arts,[2] M. C. M. van Loosdrecht,[1] J. G. Kuenen,[2] and J. J. Heijnen[1]

[1]Department of Bioprocess Technology and [2]Department of Microbiology and Enzymology, Kluyver Laboratory of Biotechnology, Julianalaan 67, 2628 BC Delft, The Netherlands

Received October 14, 1992/Accepted February 2, 1994

A rotating annular reactor (Roto Torque) was used for qualitative and quantitative studies on biofilm heterogeneity. In contrast to the classic image of biofilms as smooth, homogeneous layers of biomass on a substratum, studies using various pure and mixed cultures consistently revealed more-dimensional structures that resembled dunes and ridges, among others. These heterogeneities were categorized and their underlying causes analyzed. Contrary to expectations, motility of the microorganisms was not a decisive factor in determining biofilm homogeneity. Small variations in substratum geometry and flow patterns were clearly reflected in the biofilm pattern. Nonhomogeneous flow and shear patterns in the reactor, together with inadequate mixing resulted in significant, position-dependent differences in surface growth. It was therefore not possible to take representative samples of the attached biomass. Like many other types of reactors, the Roto Torque reactor is valuable for qualitative and morphological biofilm experiments but less suitable for quantitative physiological and kinetic studies using attached microorganisms. © 1994 John Wiley & Sons, Inc.

Key words: biofilm • biofilm reactors • structure • heterogeneity • kinetics • modeling

INTRODUCTION

Biofilms are ubiquitous and can often be a nuisance (e.g., fouling of ships, dental plaque). Biofilm research has, in recent years, expanded in an attempt to understand, predict, and influence biofilm formation. Natural biofilms are usually very complex and heterogeneous with respect to the types of microorganisms present, the physicochemical interactions occurring, and the internal and external structure of the biofilm. One way of reducing the complexity of biofilm systems in the laboratory is to use defined communities of test organisms, preferably monocultures. For modeling purposes, the system can also be simplified by reducing structural diversity, i.e., considering only one-dimensional gradients of biomass and other compounds perpendicular to the substratum surface.[1,4,14,23,33] This leads to a concept of biofilms as thin, homogeneous layers of a constant thickness that completely cover the substratum, as is implied in the name bio*film*. Such a uniform biofilm is also essential for accurate experimental determination of kinetic constants.

Although it has always been apparent that biofilms do not always fit the above concept, for example, some biofilms are patchy or filamentous,[2,8,11,13,18,26–28] comparatively little effort has been expended in describing or quantifying biofilm heterogeneity. Attempts have been made to design reactors which minimize heterogeneity, making validation of biofilm models easier.[9,15,17] One such reactor is the Roto Torque reactor,[9,17] which is essentially an adaptation of a Couette vessel. The Roto Torque reactor was selected for use in the experiments described here because it offers a well-mixed liquid phase as well as an even shear over the reactor walls, thus providing optimal conditions for homogeneous biofilm formation, which can be inspected on removable reactor wall segments (slides).[9,17] The Roto Torque reactor has also frequently been used to study biofilm physiology.[6,19,26,29]

This article describes the use of this reactor for qualitative and quantitative studies on biofilm heterogeneity. Different bacterial cultures, both motile and nonmotile, were used under both aerobic and denitrifying conditions. The type and degree of biofilm heterogeneity will be categorized, and the consequences of such heterogeneity for experiments, calculations, and modeling indicated. Finally, the usefulness of the Roto Torque reactor for biofilm studies will be discussed.

MATERIALS AND METHODS

Microorganisms

Thiosphaera pantotropha LMD 82.5 was obtained from the culture collection of the Laboratory for Microbiology and Enzymology of the Delft University of Technology. *Pseudomonas pickettii* G9 LMD 90.79 was isolated from an enrichment culture on acetate and nitrate inoculated from an anaerobic fluidized bed reactor being used for anoxic am-

* To whom all correspondence should be addressed.

© 1994 John Wiley & Sons, Inc.
CCC 0006-3592/94/020194-11

monia oxidation.[30] Stock cultures were maintained at −70°C with 30% (v/v) glycerol. Prior to further cultivation, samples from the frozen stock cultures were plated on TY agar (Oxoid tryptone, 1.6 g · L^{-1}; Difco yeast extract, 3 g · L^{-1}; Difco agar, 15 g · L^{-1}) plates. A single colony was used for overnight cultures. *Pseudomonas aeruginosa* was obtained from the collection of the Center for Biofilm Engineering, Montana State University, Bozeman, Montana.[24] Stock inocula were maintained at −70°C in 2% peptone with 20% (v/v) glycerol.

Media

The mineral medium described by van Schie et al.[31] was used in all *T. pantotropha* and *P. pickettii* G9 experiments, with the following modifications: All components were diluted fivefold and the medium was supplemented with sodium acetate (0.1 to 4 m*M*) and potassium nitrate (0.2 to 8 m*M*). The pH of the complete medium was adjusted to 8.0. Media were heat sterilized at 120°C. In the mixed-culture experiments, the same medium without nitrate was used, and the pH was adjusted to 7.5. The medium was prepared in 10-fold concentration and diluted on-line with tap water. Both medium and filter-sterilized tap water were continuously aerated. For *P. aeruginosa* the mineral medium described by Siebel and Characklis[26] was used, with the following modifications: 0.0023 mg · L^{-1} $Co(NO_3)_2 \cdot H_2O$ was added and 225 mg · L^{-1} Na_2HPO_4 was used, giving a final pH of 7.0. The medium was prepared in 32-fold concentration and autoclaved at 120°C; glucose and phosphate buffers were autoclaved separately. The medium was diluted on-line with filter-sterilized, air-saturated distilled water.

The Roto Torque Reactor

The Roto Torque reactor, a rotating annular reactor, was developed especially for biofilm studies.[9] It consists of a stationary outer cylinder and a rotating solid inner cylinder (Fig. 1). The reactor is made of autoclavable polycarbonate. Twelve removable polycarbonate slides are fitted into the outer cylinder inside wall, allowing biofilm sampling. Access to the slides is through ports closed with rubber stoppers on top of the reactor. Rotation of the inner cylinder causes a shear field in the reactor independent of the medium flow. Draft tubes in the inner cylinder create an internal liquid circulation when rotating, enhancing mixing. The system can therefore be described as a continuous flow stirred tank reactor (CFSTR). The reactors were obtained from the Center for Biofilm Engineering, Montana State University, Bozeman, Montana. Reactor dimensions are given in Table I.

Mixing Studies

The general mixing behavior of the reactor was determined by measuring the effluent conductivity after a stepwise change in influent salt concentration from 0 to 0.1 or 0.01 *M* NaCl for (i) different rotational speeds (100 to 300 rpm) and (ii) different combinations of influent and effluent port positions at the top and bottom of the reactor. Ninety-five percent mixing times for a series of rotational speeds (50 to

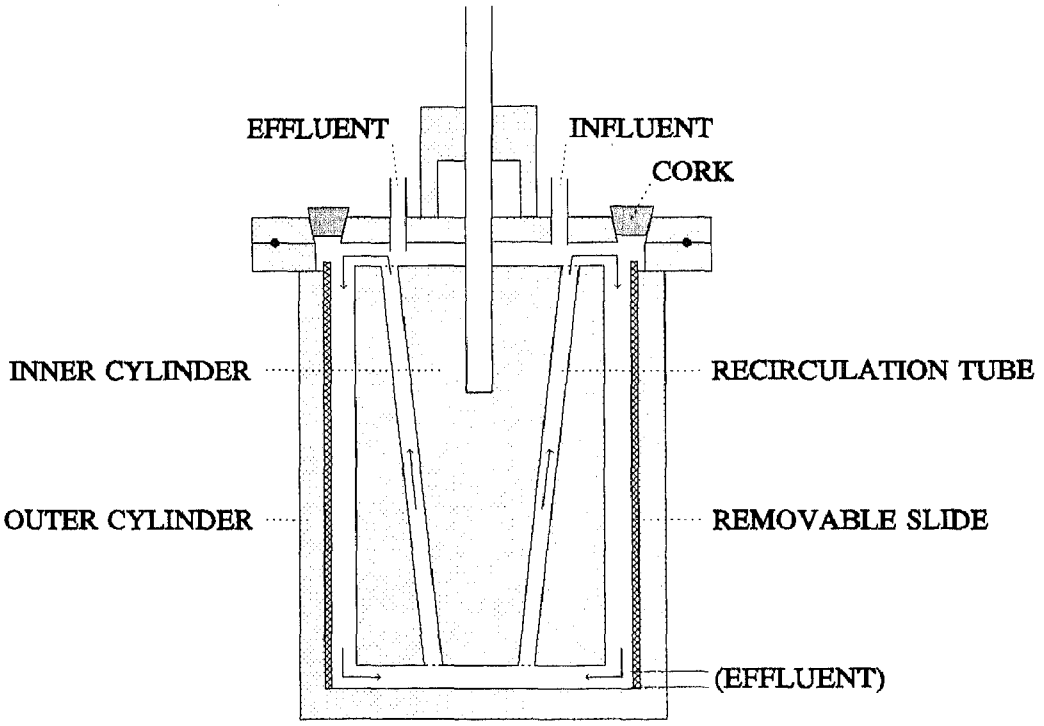

Figure 1. Schematic representation of a Roto Torque reactor.

Table I. Characteristics of the two Roto Torque reactors used in the experiments.

Parameters	Reactor 1	Reactor 2
Diameter of inner cylinder (mm)	100.5	100.8
Diameter of outer cylinder (mm)	116.6	115.7
Width of annular gap (mm)	8.05	7.45
Wet height of inner cylinder (mm)	175.5	176.5
Wet height of outer cylinder (mm)	189.2	192.5
Wet length of slide (mm)	188.3	191
Width of slide (mm)	17.0	17.0
Total wet surface area (m^2)	0.18	0.18
Working volume (L)	0.67	0.67
Surface volume ratio ($m^2 \cdot m^{-3}$)	0.27	0.27
Total slide surface area (%)	21.1	21.2
Annular area of outer cylinder (%)	38.0	38.1
Annular area of inner cylinder (%)	30.4	30.5
Area of bottom, drafts, and top (%)	31.6	31.4

500 rpm) were determined in pulse response measurements by injecting 0.3 mL 2 *M* H_2SO_4 into a reactor filled with demineralized water. To monitor the pH, a pH electrode connected to a recorder was fixed in the top part of the reactor through one of the slide sampling ports.

Operation of the Roto Torque Reactor

The reactor was autoclaved at 110°C for 30 min. For the *P. aeruginosa* experiments, the reactor was kept at 24°C. The rotational speed was 150 rpm. The lowest port on the reactor was used for effluent removal. The reactor was inoculated by injecting 1 mL concentrated *P. aeruginosa* stock inoculum into the medium-filled reactor and operating it in the batch mode for 24 h. Subsequently, the dilution rate was set at 3 h^{-1}.

For experiments involving *T. pantotropha, P. pickettii* G9, and mixed cultures, some modifications in the reactor setup were made. The influent and effluent ports were both located at the top of the reactor. To facilitate removal of the effluent, the reactor was kept under 0.1 atm overpressure with sterilized air or nitrogen gas. The temperature was kept at 30°C. The rotational speed was 150, 200, or 250 rpm (Table II). For denitrifying growth (*T. pantotropha* and *P. pickettii* G9), the reactor was fitted with Norprene tubing to avoid diffusion of oxygen, and the medium reservoir was continuously sparged with nitrogen gas. The reactors were inoculated from overnight batch cultures, and experiments were started at a low dilution rate (typically 0.15 h^{-1}). After a steady state had been reached, the dilution rate was increased to 1.0 or 1.2 h^{-1}. Experiments with undefined mixed cultures were initially inoculated with *T. pantotropha*, and aseptic conditions were not maintained. In one of the mixed-culture experiments, some of the slides were roughened. Four slides were treated with emery paper No. 600 (Carbimet silicon carbide grinding paper), creating scratches of 30 μm wide and 5 μm deep, and four slides with emery paper No. 400, creating scratches of 45 μm wide and 7.5 μm deep. Of both groups, two slides were given scratches perpendicular and two slides scratches parallel to the direction of the flow in the reactor.

In all experiments, effluent samples were taken daily. Biofilm samples were also taken daily or, for some of the pure culture experiments, only at the end of the experiment in order to reduce the risk of contamination.

Analytical Procedures

The purity of the cultures was routinely checked by plating on TY, GTY (glucose, 20 $g \cdot L^{-1}$; Oxoid tryptone, 20 $g \cdot L^{-1}$; Difco yeast extract, 10 $g \cdot L^{-1}$; Difco agar, 15

Table II. Growth characteristics and structure of biofilms grown in Roto Torque reactors.

Experimental conditions						Biofilm structures						
						Gradient in thickness						
Microorganism	Motility	Carbon source	Carbon load ($mmol \cdot m^{-2} \cdot h^{-1}$)	Oxygen	*N* (rpm)	Horizontal	Vertical	Patchy	Lines	Dunes	Comets	Filament
Mixed culture	nd	ac	1.2	+	200	+	+	+	±	−	−	−
Mixed culture	nd	ac	1.2	+	200	+	nd	+	+	−	+	−
Mixed culture	nd	ac	1.2	+	200	+	nd	+	nd	−	−	+
Mixed culture	nd	ac	1.2	+	200	+	+	+	+	−	−	+
P. aeruginosa	+	gluc	6.9	+	150	nd	nd	−	nd	+	−	−
P. aeruginosa	+	gluc	8.0	+	150	nd	nd	−	+	+	−	−
P. aeruginosa	+	gluc	6.9	+	150	+	+	−	+	+	−	−
T. pantotropha	−	ac	37.0	−	250	+	+	+	±	−	−	+
T. pantotropha	−	ac	37.0	−	150	+	+	+	±	−	−	+
T. pantotropha	−	ac	19.0	−	150	+	+	+	±	−	−	+
T. pantotropha	−	ac	1.9	−	250	+	+	+	±	−	−	+
P. pickettii	+	ac	1.9	−	250	+	+	+	−	−	−	−
P. pickettii	+	ac	1.9	−	150	+	+	+	−	−	−	−
P. pickettii	+	ac	37.0	−	150	+	+	+	−	−	−	−
P. pickettii	+	ac	0.9	+	150	+	+	+	−	−	−	−

Note: +, present; −, not present; ±, not clear; nd, not determined; ac, acetate; gluc, glucose

$g \cdot L^{-1}$), or Difco R2A agar plates and by phase-contrast microscopy.

Acetate was determined by high-performance liquid chromatography (HPLC) using an Aminex HPX-87H column (300 × 7.8 mm, Bio-Rad) or enzymatically using a commercial test kit (Boehringer). Glucose concentrations were determined enzymatically (Sigma Diagnostics glucose oxidase kit).

To determine viable cell numbers, cell suspensions were homogenized (Tekmar Tissumiser, 1 min), dilution series were made in sterile phosphate buffer (226 mg $\cdot L^{-1}$ Na_2HPO_4 and 205 mg $\cdot L^{-1}$ KH_2PO_4) and were plated on R2A agar. Plates were incubated at 30°C for 1 day and the colonies counted. Biofilm cell suspensions were prepared by scraping biofilm (Costar disposable cell scraper 3010) aseptically from one of the wall slides into 30 mL sterile phosphate buffer.

The dry weight of culture samples was determined by filtering culture samples over preweighed nitrocellulose filters (pore diameter 0.45 μm, Schleicher and Schüll, Dassel, Germany). The cells were washed three times with demineralized water and dried to constant weight in a microwave oven (15 min at 180 W output). Biofilm dry weight was determined from the weight difference of dried wall slides with and without biofilm.

For the determination of total organic carbon, cell suspensions were centrifuged at 10,000 rpm and resuspended in 10 mL Millipore water before being analyzed in a Tocamaster (Beckmann).

The morphology of the biofilms on slides from the wall of the Roto Torque reactor was studied using an Olympus SZH-ILLD stereo microscope with additional illumination (Olympus Highlight 2000) and by phase-contrast or dark-field microscopy using an Olympus BH2 microscope. Pictures were taken using an Olympus PM-10ADS camera.

Biofilm thickness was measured by optical microscopy as described by Bakke and Olsson,[7] multiplying the micrometer reading by 1.34, the quotient of the refractive indexes of water and air.[27] Averages of at least eight measurements were used.

RESULTS

Mixing Properties of the Roto Torque Reactor

To obtain homogeneous biofilm formation, it is necessary that the liquid phase in the biofilm reactor is without gradients, i.e., well mixed. The mixing characteristics of the Roto Torque reactor were therefore determined using step and pulse response measurements. The response to a stepwise change in influent sodium chloride concentration closely followed the theoretical curve of an ideally mixed reactor (Fig. 2). Different positioning of influent and effluent ports (top/top or top/bottom) did not influence this result. The mixing time (t_m), as determined by the response to a pulse addition of sulfuric acid, decreased with increasing rotational speed (N) (Fig. 3). The shortest liquid residence

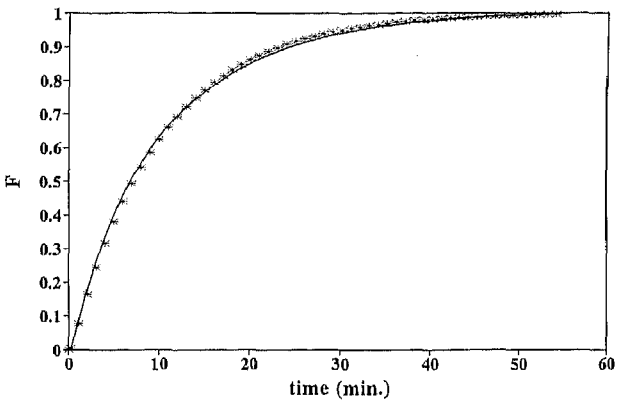

Figure 2. Dimensionless salt concentration (F) in Roto Torque effluent after a stepwise change in influent salt concentration (0 to 0.1 M NaCl) (N = 250 rpm): (*) measured data; (⁻) calculated curve assuming ideal mixing.

time during the growth experiments was 20 min. This is much longer than the mixing time (30 s) measured at the lowest rotational speed (150 rpm) used in the growth experiments. On the basis of these criteria, the system can be considered to be ideally mixed. Above a rotational speed of 100 rpm, the product $N \cdot t_m$ was approximately constant, indicating turbulent flow.

Biofilm Morphology

Biofilm growth experiments in the Roto Torque reactor were conducted with pure cultures and with undefined mixed cultures. An overview of the experiments carried out during this study is given in Table II. Smooth biofilms were not observed during any of these experiments. Instead, a variety of different biofilm structures were observed (Table II and below).

Microorganism-Related Biofilm Structures

The structure of the biofilm varied with the bacterial species being tested. In the case of *T. pantotropha*, rapid biofilm

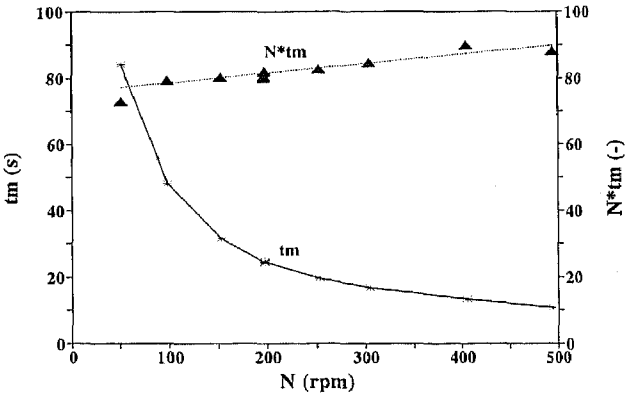

Figure 3. Mixing time (95%) as function of rotational speed in the Roto Torque reactor.

growth was observed after increasing the dilution rate above the maximum specific growth rate of the organism. This growth appeared as microcolonies, with empty space between them. Even after prolonged cultivation (3 weeks), microscopy revealed a patchy appearance (Figs. 4a and 4b). This phenomenon was also observed with some of the mixed cultures. In several runs with *T. pantotropha* or mixed cultures, the microcolonies evolved into filamentous structures (Fig. 4c). Filament formation was particularly evident during cultivation at high substrate loads. Anoxic cultures of *P. pickettii* G9 formed a very thin base film with microcolonies on top. After prolonged cultivation, these biofilms still retained their patchy appearance. *P. aeruginosa* developed into relatively smooth biofilms. However, even with this organism, the biofilms were not entirely homogenous, as will be discussed below.

Surface-Related Biofilm Structures

Some of the inhomogeneities observed in the biofilm appeared to correlate with the structure of the substratum. In one of the mixed cultures, comet-like biofilm patterns were observed (Fig. 5). These originated at unevennesses at the surfaces and/or sides of the removable slides and became both wider and thinner in the direction of the flow. It was noted that even unused polycarbonate slides were scratched and further damage during cleaning was unavoidable. In most of the experiments, the effect of these small, shallow scratches (<0.5 μm) on biofilm morphology was not obvious as they did not interact with the pattern of biofilm formation. When slides were deliberately roughened with emery paper, creating scratches with widths of 30 to 45 μm and depths of 5 to 7.5 μm, significantly more biomass attached (23 ± 2 mg · m^{-2} DM) than on the untreated slides (17 ± 2 mg · m^{-2} DM). No difference was found between slides roughened with different grades of emery paper. There did not appear to be any relationship between the orientation of the scratches relative to the direction of the flow and biomass accumulation.

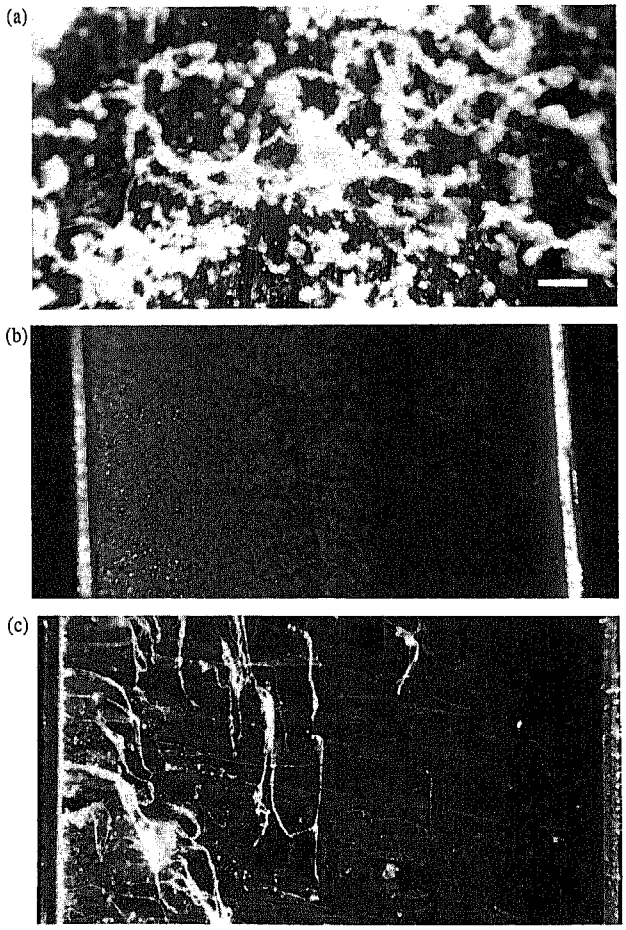

Figure 4. Different examples of nonhomogeneous biofilms on the Roto Torque slides: (a) patchy (*T. pantotropha*), bar = 0.5 mm; (b) microcolonies (*T. pantotropha*); (c) filamentous (mixed culture). The decrease in biofilm density in the direction of the flow (left to right) can be clearly observed.

Flow-Related Biofilm Structures

The biofilms generally formed a pattern of lines on the sampled slides and on the inner and outer cylinder walls of the reactor (Fig. 6a). The lines appeared to follow the direction of the flow, in the annulus slightly inclining from the horizontal drum rotation. The change in flow direction of the circulating bulk liquid at the top and bottom of the reactor was reflected in the changing inclination of the line pattern. At the top of a slide with *P. aeruginosa* biofilm, the inclination was more than 40° and decreased to 7° over the first few centimeters downward as the liquid entering the annulus caught up with the drum rotation. On the bottom of the outer cylinder, the line pattern spiraled toward the center, where the liquid entered the draft tubes (Fig. 6b).

These line patterns could be divided into two groups on the basis of their size and spacing. In mixed cultures, sampled after 14 days of cultivation and over, the lines were approximately 1 mm apart and usually rather irregular. In young *P. aeruginosa* biofilms (3 to 4 days), the pattern was much finer, about 20 μm apart, and more regular (Fig. 7a).

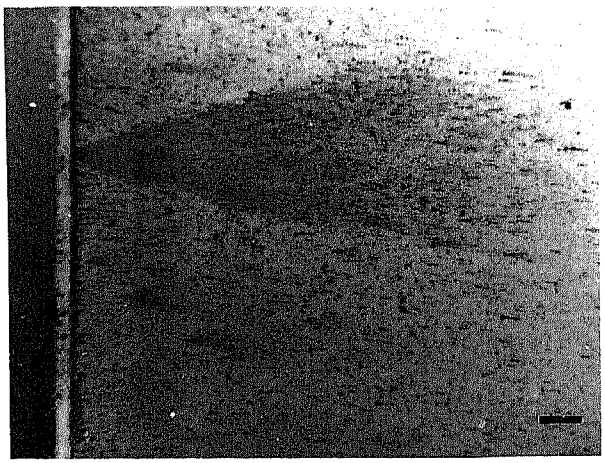

Figure 5. Comet-like patterns in a mixed-culture biofilm. Bar = 1 mm.

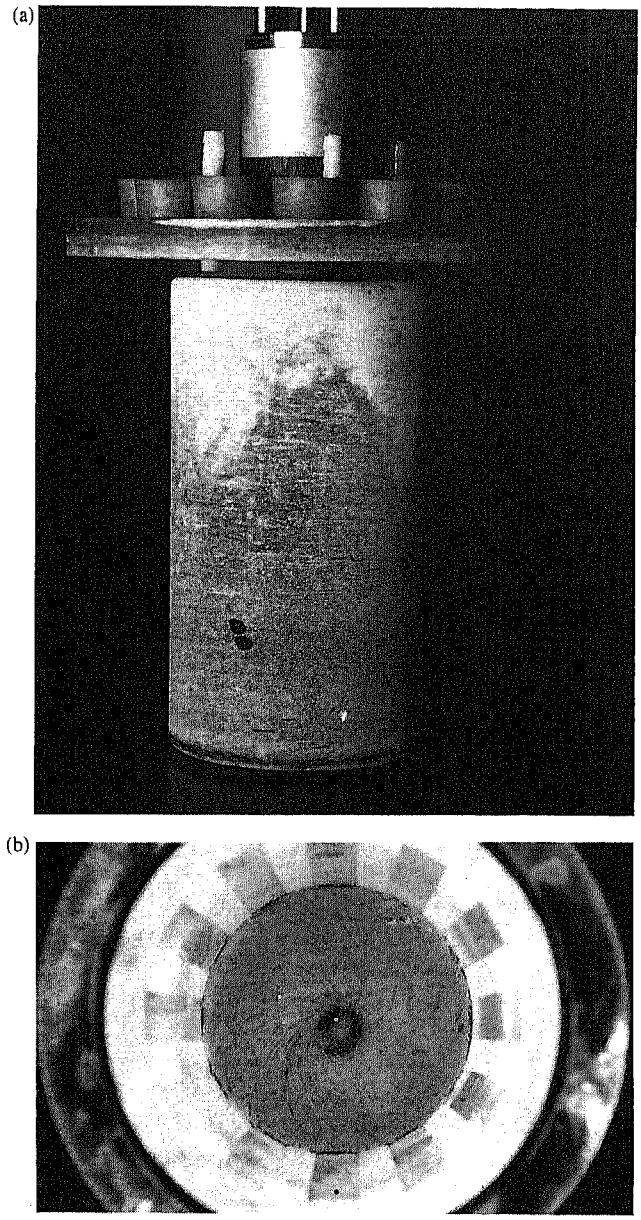

Figure 6. Spatial biofilm inhomogeneity in the Roto Torque: (a) inner cylinder with vertical thickness gradients and horizontal line patterns; (b) bottom of the outer cylinder with spiralling line pattern.

In very early *P. aeruginosa* biofilms (2 days) a line pattern was not evident, suggesting that a minimum film thickness if required. In older and thicker *P. aeruginosa* biofilms (5 days and over), the pattern was replaced by dune-like ridges perpendicular to the flow direction (Fig. 7b). These ridges were about 90 μm apart and 20 μm high. These ridges can probably be described by a sinusoid surface, because the minimum and maximum values obtained in a series of thickness measurements correlated very well with the average $\pm 2^{0.5} \times$ standard deviation, which gives the minimum and maximum of a sinus function (Fig. 8). In addition to these ridges, a pattern of larger, irregular dunes with a spacing of 0.1 to over 0.2 mm was observed on part of the slides (Fig. 7c).

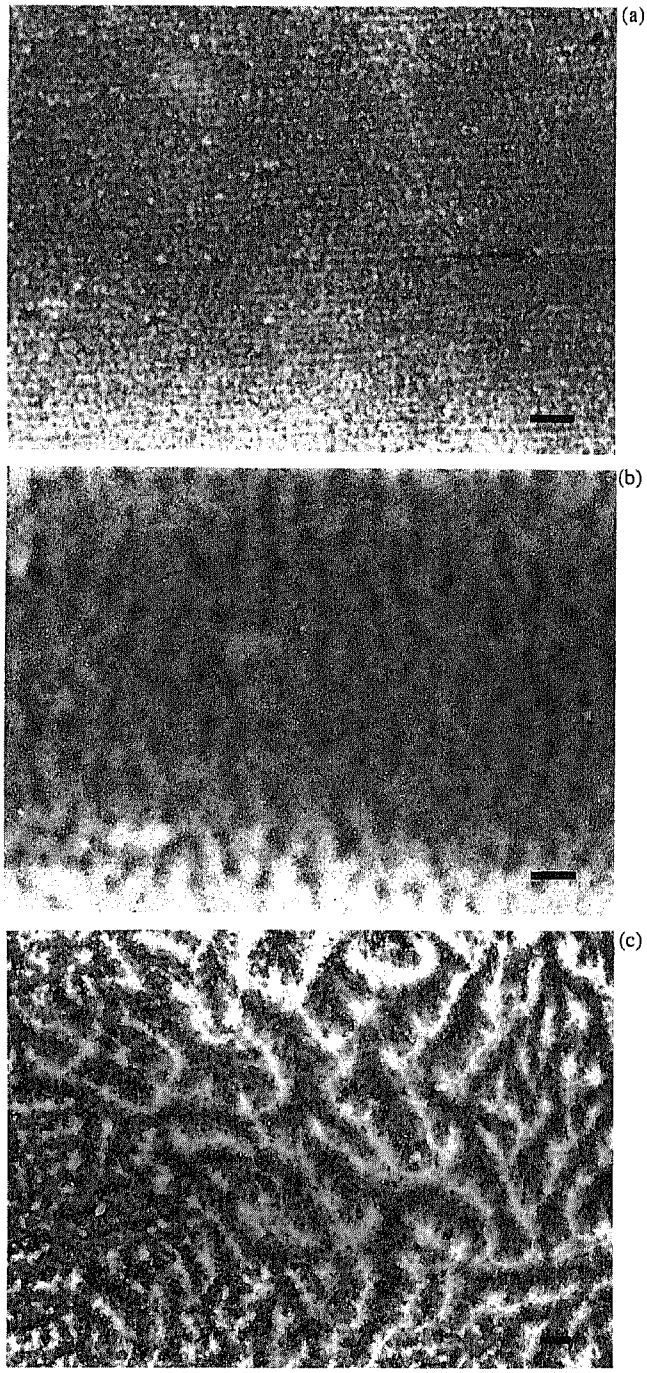

Figure 7. Different patterns in *P. aeruginosa* biofilms: (a) line pattern (t = 4 days); (b) transversal ridges (t = 6 days); (c) dunes (t = 6 days). Bar = 100 μm.

Reactor-Related Inhomogeneities

In all experiments, biofilm formation started at the upstream side of the slides and interspaces, and the amount of biomass decreased in the direction of the flow. The difference between upstream and downstream sides became more and more pronounced during biofilm development, leading to very large thickness differences in steady-state biofilms (Figs. 4b, 4c, and 9), especially at higher substrate loading rates.

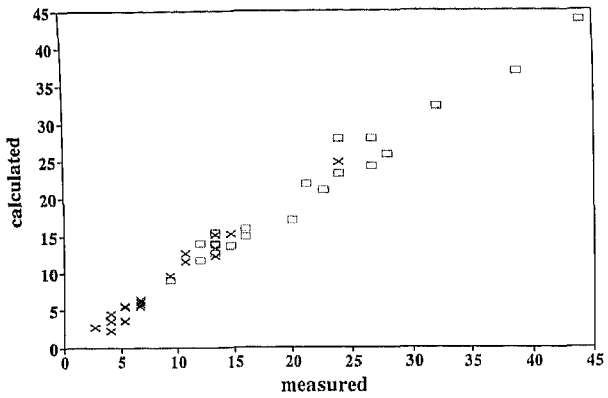

Figure 8. Parity plot of (x) minima and (□) maxima values in different series of optical thickness measurements of *P. aeruginosa* biofilm grown in a Roto Torque reactor. Calculated values are based on the assumption of a sinusoidal surface.

Large differences were also found in the vertical direction (Table III). The biofilm in the upper part of the reactor was consistently thicker and/or denser than in the lower part of the reactor and less susceptible to sloughing. This vertical gradient also appeared on the inner cylinder (Fig. 6a). Another important observation was the large difference in biofilm thickness between different slides taken from the same reactor at the same time and between the slides and the interspaces of the outer cylinder wall. Biofilm on the interspaces was more homogeneous and less susceptible to sloughing.

Sloughing-Related Biofilm Structures

During most of the experiments, large patches of the biofilm periodically sloughed off. With *P. aeruginosa*, sloughing usually started after 5 or 6 days, when the biofilm approached its maximum thickness. Sloughing always started at the upstream side of the slides and interspaces, leaving behind a relatively thin and rather homogeneous layer of biomass (Fig. 10). Biofilm in the lower part of the reactor

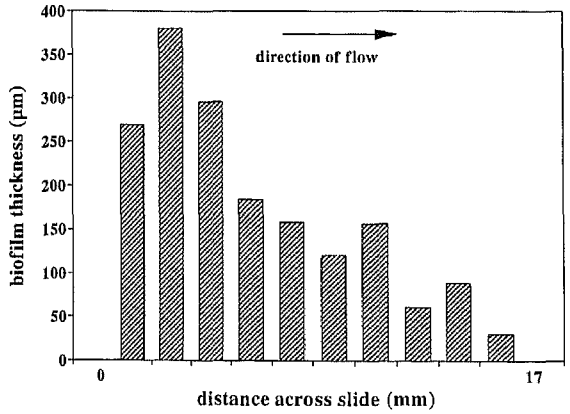

Figure 9. Variations of thickness of a patchy *T. pantotropha* biofilm on a Roto Torque slide in the direction of the flow (single measurements).

Table III. Amount of biomass from a mixed-culture biofilm on different surfaces in the Roto Torque reactor.

Surface	Total organic carbon (mg C · m^{-2})
Slide, whole	420
Slide, upper part	460
Slide, lower part	138
Inner cylinder	443

was more susceptible to sloughing than in the upper regions.

DISCUSSION

The growth of biofilms in the Roto Torque reactor has frequently been assumed to be homogeneous. This research, together with several other recent publications,[2,8,11,13,18,26–28] indicates that biofilms will always have some inhomogeneities. Possible causes and consequences of this will be discussed below.

Possible Causes of Biofilm Inhomogeneities

Motility

It has been suggested that motility may be important for microorganisms to be able to form homogeneous biofilms covering the available surface area. Siebel[26] showed that *P. aeruginosa*, a motile organism, attached to polycarbonate in a relatively uniform distribution, growing into a smooth biofilm, while *Klebsiella pneumoniae*, a nonmotile organism, formed tower-like clusters with bare substratum in between. Korber also described how the spatial distribution of adhering cells was influenced by motility.[16] Motile cells dispersed over surfaces more uniformly than nonmotile cells, allowing uniform biofilm development. In this context, nonmotile organisms such as *T. pantotropha* would be

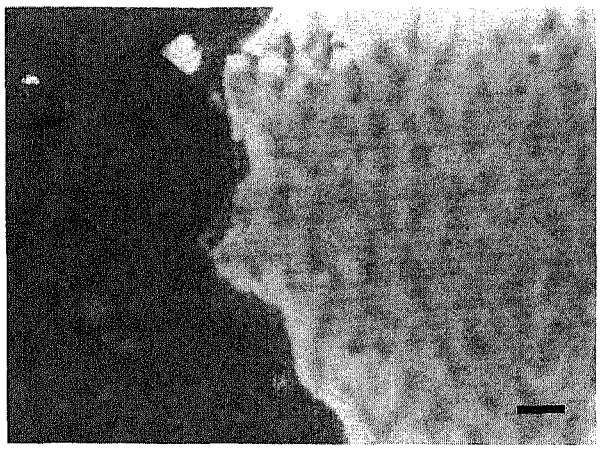

Figure 10. Sloughing of a *P. aeruginosa* biofilm starting at the upstream side of a Roto Torque slide (flow from left to right). Bar = 100 μm.

expected to form microcolonies or patchy biofilms, whereas motile organisms (*P. pickettii* G9 and *P. aeruginosa*) should form homogeneous biofilms. However, in the work described here, the motile organisms also formed inhomogenous biofilms, indicating that motility does not guarantee homogeneous biofilms.

Surface Roughness and Flow

Correlation between the roughness of the substratum surface and cell adhesion and biofilm formation has often been reported. Pedersen[21] found 1.4 times more microcolonies on matted steel than on electropolished steel after exposure to running municipal drinking water for 167 days. Quirynen and co-workers[22] reported that the rate of bacterial colonization of intraoral hard surfaces and the rate of plaque maturation were positively correlated with surface roughness. This supports our observation that the biomass accumulation on roughened polycarbonate was higher than on smooth polycarbonate. The rough surface may provide shelter against shear forces for adsorbed and attached cells, reducing detachment.[10,32] A minimum degree of roughness in the order of one cell diameter might be needed to provide sufficient shelter, as small and shallow scratches (<0.5 μm) were found to not promote biomass accumulation.

Similarly, local irregularity may offer cells protection against shearing. Verran and co-workers[32] observed that *Candida albicans* cells adhered between surface ridges, often in clumps, and often to any debris present. The comet-like biofilm patterns shown in Figure 5 appeared to originate at irregularities on the surfaces and sides of the polycarbonate slides. Their shape strongly suggests a direct interaction between liquid flow and biofilm accumulation. If debris and surface irregularities can enhance local biomass accumulation, separate microcolonies might do the same. This might then result in lines and stripes of thicker biofilm in the direction of the flow, as described above (Figs. 6 and 7a). A similar line pattern was shown by Capdeville and Nguyen.[8] Similarly, Pedersen[21] observed bacteria growing in patchy microcolonies in the direction of the flow, and Santos et al.[25] also reported the alignment of a *Pseudomonas fluorescens* biofilm in the direction of the liquid flow. The ridges and dunes (Figs. 7b and 7c) also suggest an interaction between flow and biomass, though the mechanism is harder to explain. A parallel might be found in desert sands, where small variations in a combination of factors such as grain size distribution, grain density, wind velocity, and wind direction can lead to very different patterns of sand dunes.[5]

Reactor Mixing

In most of the runs it was observed that the biofilm decreased in thickness as its distance from the top of the reactor increased. This could have been caused by a decrease in the width of the annular gap toward the bottom, resulting in increasing shear stress on the walls. Careful measuring of the inner and outer cylinder ruled out this option. Another cause could be the uneven distribution of nutrients in the reactor. The substrate was added at the top of the vessel. As the substrate is growth limiting, concentration gradients could easily form. Tracer studies showed that the reactor was well mixed on the macroscale (Fig. 2), and the mixing time was much smaller than the hydraulic residence time. This, however, does not imply that the reactor was also well mixed on the microscale. The conversion of consumable substrates must be taken into account. The characteristic times for substrate conversion during two of the experiments were therefore calculated (see Table IV). These appear to be of the same order of magnitude as the mixing time. Characteristic uptake times smaller than or equal to the mixing time strongly indicate that the uptake of substrate is as fast or faster than the mixing in the reactor. This will result in concentration gradients, because biomass located close to the influent port will be able to consume more substrate. A thicker biofilm will thus be formed close to the influent port. This was also observed by Arcangeli and Arvin[2] in a comparable reactor system. Localized depletion may occur lower in the reactor. Sloughing, a phenomenon commonly believed to be linked to substrate or oxygen depletion, was greater in the lower regions of the reactor.

Reactor Geometry

In addition to vertical thickness gradients, a horizontal decrease in thickness of the biofilm on each individual slide in the direction of flow was observed. This horizontal gradient can probably be explained by the local geometry of the reactor: Whereas the outer cylinder has a curved surface, the inserted slides are flat, cutting off part of the curvature

Table IV. Physiological parameters and chracteristic times for substrate uptake and mixing[a].

Parameters	*T. pantotropha*	*P. aeruginosa*
N (rpm)	150	150
V (L)	0.67	0.65
$X_s \cdot V$ (mg)	43	3.5[d]
$X_f \cdot A$ (mg)	460	38[d]
μ (h^{-1})[a]	0.1	0.074
D (h^{-1})	1.2	3.0
S_i (mg · L^{-1})	240	15.7
S (mg · L^{-1})	1.2[b]	2
Y_{XS} (g · g^{-1})[a]	0.27	0.41[c]
t_{s1} (s)[a]	15	175
t_{s2} (s)[a]	16	181
t_m (s)	32	32

[a] $t_{s1} = S/D(S_i - S)$ $t_{s2} = Y_{XS} \cdot S \cdot V/\mu(X_s \cdot V + X_f \cdot A)$
$\mu = X_s \cdot V \cdot D/(X_s \cdot V + X_f \cdot A)$

[b] Residual acetate concentration is 1.2 mg · L^{-1} (determined in continues culture).

[c] From ref. 24.

[d] Recalculated from cfu · m^{-1} and cfu · m^{-2} using cell volume 10^{-12} cm^3, cell density 1.07 g · cm^{-3} (ref. 12) and dry weight 25% (ref. 20).

and narrowing the annual gap (Fig. 11) by as much as 8% (0.6 mm). This will strongly influence the flow and the shear in that area and consequently affect the deposition and removal of cells on the surface of the slide. Moreover, the disruption of the homogeneous flow of medium due to the flat slide might result in differences in external diffusion gradients between biofilm surface and bulk liquid. This can also affect the horizontal biofilm accumulation.

Consequences of Inhomogeneity

Surface Area Enlargement

Biofilm inhomogeneity will, in most cases, increase the contact area between bulk liquid and biofilm. Using simple approximations, this surface increase can be estimated for some biofilms. A biofilm with a line structure or with ridges can, for example, be described by a sinusoid plane. Using line integration for such a plane with amplitude 1 $\{(x, y, z) = (x, y, \sin y)\}$, enlargement of the interfacial area by a factor of 1.2 is obtained. This factor increases with the amplitude of the sinuses. If the biofilm consists of a base film with filaments extending into the bulk liquid, the surface enlargement depends on the number and size of the filaments. Assuming the filaments are all of the same diameter d and length ℓ and have a density of n filaments per unit area of substratum, the enlargement factor E is given by $E = 1 + n \cdot \ell \cdot d \cdot \pi$. The number of filaments in the biofilm shown in Fig. 4c was estimated to be approximately 0.3 mm^{-2}, most filaments being 5.5 mm long and 0.1 mm in diameter, giving a surface enlargement of 1.5. If the filaments are longer, thinner, or more numerous, the enlargement factor increases. A denser filamentous biofilm, described by Kugaprasatham et al.,[18] gave an 11-fold estimated enlargement ($n = 32$ mm^{-2}, $\ell = 1$ mm, $d = 0.1$ mm). Only when a biofilm is patchy and discontinuous, as is the case when a "film" consists of separate colonies (Fig. 4b), the surface of the biofilm–bulk interface will be smaller compared to a homogeneous layer containing the same amount of biomass.

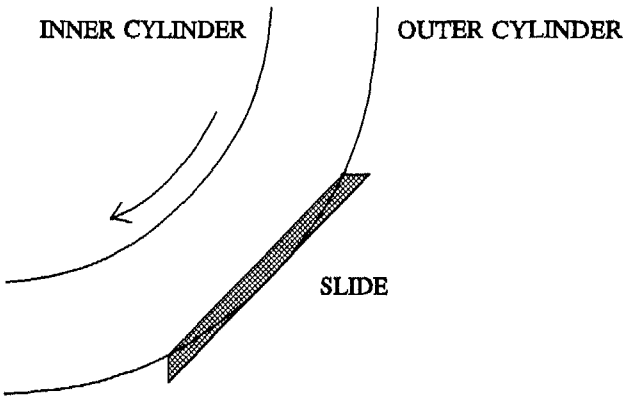

Figure 11. Schematic representation of a Roto Torque slide cutting off part of the curvature in the annular gap.

These theoretical exercises show that the increase or decrease in the interfacial area can be quite considerable. However, in practice it will not be possible to determine this factor within reasonable limits of accuracy, because the very diverse morphology prevents simple mathematical description. The increase in the interfacial area cannot be estimated, because direct measurements either give averages over sampled areas (e.g., dry weight) or give unrelated local values (thickness measurements).

Mass Transfer

A larger contact area will facilitate external mass transfer between the bulk liquid and the biofilm. A rough surface can also improve external mass transfer by increased eddy diffusion[27] and fluttering filaments.[18] More active biomass may therefore be present than might be expected from the dimensions of the reactor system. The biofilm surface exposed to shear will also be larger. The effect of this on the net biofilm accumulation is hard to predict as both detachment and attachment rates may increase.

Within the biofilm, mass transfer may be negatively affected. Because of the inhomogeneity, localized areas of biofilm may be much thicker than average. Should the average thickness correspond with the penetration depth of the rate-limiting substrate, then the deeper regions of the thicker parts may become substrate limited (Fig. 12). In this way, anaerobic sites can occur in an aerobic biofilm, even when this is not predicted from the average biofilm thickness. This can especially be true when large-scale systematic differences in thickness occur, such as the horizontal thickness gradients observed on the Roto Torque slides. Local depletion of substrate or oxygen would explain the sloughing at the upstream side of the slides where the biofilm was the thickest.

Kinetics and Modeling

As discussed above the surface area and amount of active biomass in a heterogeneous biofilm cannot be measured. It is therefore not possible to accurately determine specific substrate consumption rates using the difference between influent and effluent substrate concentration measurements (e.g., substrate removed per amount of biomass per unit of time). Biofilm heterogeneity also affects mass transfer inside the biofilm. Since substrate concentration is a key factor in the physiology of microbial cells, the position of an individual cell in the biofilm will affect not only its growth (and thus the amount of biomass) but also its physiological properties. Calculated kinetic parameters will therefore be system dependent and cannot be used as a general value.

Common biofilm models do not take more-dimensional biofilm heterogeneity into account,[1,4,14,23,33] and they use parameters from heterogeneous biofilms that have no general value. Thus the results from such models only relate to the particular system and cannot be generalized.

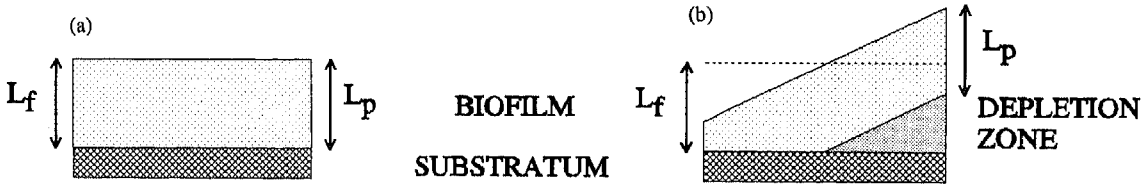

Figure 12. Illustration of substrate depletion inside a biofilm due to biofilm inhomogeneity: (a) homogeneous biofilm; (b) nonhomogeneous biofilm of equal average thickness (L_f) (L_p = substrate penetration depth).

Limitations of the Roto Torque

The Roto Torque has been described as a suitable laboratory system for monitoring biofilm development,[9] in which most of the surface area is exposed to a uniform shear stress. However, closer examination of the Roto Torque indicates that shear stress on the walls of the bottom and top of the reactor, as well as in the recirculation tubes (together accounting for approximately 30% of the reactor surface, see Table I), will differ from the shear in the annular gap, because of different flow patterns and velocities. In the upper and lower parts of the annular region, the flow direction changes. Approximately 2 cm from the top and bottom of the outer cylinder is needed for the flow to become homogeneous. This increases the amount of reactor surface where shear stress differs from that in the main part of the annular gap to 38%.

The torque at the inner and outer cylinder walls of the annular gap is the same. The shear stress τ relates to the torque via the inverse square radius (R), giving $\tau_i/\tau_o = R_o^2/R_i^2 = (R_i + (R_o - R_i))^2/R_i^2$ (i = inner, o = outer). Thus the shear stress on both surfaces can only be considered to be equal when the width of the annular gap is small compared to the radius of the cylinders. In the Roto Torque, this gap is relatively wide, resulting in significant differences in shear stress: $\tau_i/\tau_o = 1.3$. Two surfaces remain that could possibly be under homogeneous, but distinct, shear stress. However, the flat removable slides in the outer cylinder wall interrupt its curvature (Fig. 11) and disturb the flow field near the wall. This explains the biofilm thickness gradient in the direction of flow consistently observed on all slides (Figs. 4b, 4c, and 9). A homogeneous shear field can therefore only be expected over the inner cylinder annular wall. This accounts for only 30% of the total biofilm area and does not include the surfaces from which biofilm samples can be taken.

The data presented here demonstrate that the biomass per unit area of sampling slide is not representative of the entire reactor surface area. Moreover, biofilm on the various slides was not the same and large gradients have been found on single slides. Since it is not possible to obtain representative biofilm samples from the Roto Torque, this reactor is not suitable for use in quantitative physiological or kinetic biofilm studies (e.g., determination of maintenance energy requirement or substrate saturation constants) where it is essential that the total amount of active biomass in the system can be measured. The reactor may still be used for morphological and "black-box" biofilm studies.

The problems that have been encountered with the Roto Torque are not unique to this type of reactor. For example, in flow cells and tubular reactors, substrate gradients and inhomogeneous shear might also be hard to avoid. Experiments have indicated that in laboratory-scale airlift and fluidized bed biofilm reactors,[3] attachment to the reactor walls and tubing, as well as nonrepresentative sampling, can also hinder quantitative physiological studies. The development of novel, more suitable biofilm reactors is essential for the quantitative comparison of the physiological and kinetic properties of suspended and attached microorganisms.

We are grateful to the late W. G. Characklis of the Center for Engineering, Montana State University, Bozeman, Montana, for his hospitality and introduction in the use of the Roto Torque reactor. We are very much indebted to L. A. Robertson for discussion and helpful review of the manuscript and to P. Bos for his constructive comments. We thank Pieter Elzinga and Anke de Bruijn for their experimental assistance on this project.

Part of this research was supported by the Integrated Water Management Working Group of the Delft University of Technology, project number 89-STM-W-8, and by the NOVEM, project number 51120/0210. Furthermore the Institute for Inland Water Management and Waste Water Treatment RIZA and the Foundation of Water Research STORA sponsored the research within the framework of Future Treatment Technologies for Municipal Waste Waster in the Netherland: RWZI 2000, project 3244/3.

NOMENCLATURE

A	substratum surface area (m^2)
D	dilution rate (h^{-1})
d	average filament diameter (m)
E	biofilm surface enlargement factor (dimensionless)
F	dimensionless concentration (dimensionless)
L_f	average biofilm thickness (m)
L_p	substrate penetration depth (m)
ℓ	average filament length (m)
N	rotational speed (rpm)
n	number of filaments per unit substratum area (m^{-2})
R_i	radius inner cylinder (m)
R_o	radius outer cylinder (m)
S	substrate concentration ($g \cdot m^{-3}$)
S_i	influent substrate concentration ($g \cdot m^{-3}$)
t	time (s)
t_m	mixing time (s)
t_s	characteristic substrate uptake time (s)
V	reactor volume (m^3)
X_f	biofilm areal biomass concentration ($g \cdot m^{-2}$)
X_s	suspended biomass concentration ($g \cdot m^{-3}$)
Y_{XS}	yield ($g \cdot g^{-1}$)

Greek letters

μ growth rate (h^{-1})
τ shear stress ($N \cdot m^{-2}$)

References

1. Andrews, G. F. 1992. Aerobic wastewater process models. pp. 409–440 In: K. Schügerl (ed.), Biotechnology, vol. 4: Measuring, modelling and control, 2nd revised edition. VCH, Weinheim.
2. Arcangeli, J. P., Arvin, E. 1992. Toluene biodegradation and biofilm growth in an aerobic fixed-film reactor. Appl. Microbiol. Biotechnol. **37**: 510–517.
3. Arts, P. A. M., Robertson, L. A., Bos, P., Kuenen, J. G. 1992. Growth of *Thiosphaeara pantotropha* in a continuous-flow stirred tank reactor. Water Sci. Technol. **26**: 2177–2180.
4. Arvin, E., Harremoës, P. 1990. Concepts and models for biofilm reactor performance. Water Sci. Technol. **22**: 171–192.
5. Bagnold, R. A. 1941. The physics of blown sand and desert dunes. Methuen, London.
6. Bakke, R., Trulear, M. G., Robinson, J. A., Characklis, W. G. 1984. Activity of *Pseudomonas aeruginosa* in biofilms: Steady state. Biotechnol. Bioeng. **26**: 1418–1424.
7. Bakke, R., Olsson, P. Q. 1986. Biofilm thickness measurements by light microscopy. J. Microbiol. Meth. **5**: 93–98.
8. Capdeville, B., Nguyen, K. M. 1990. Kinetics and modelling of aerobic and anaerobic film growth. Water Sci. Technol. **22**: 149–170.
9. Characklis, W. G. 1990. Laboratory biofilm reactors. pp. 55–89 In: W. G. Characklis and K. C. Marshall (eds.), Biofilms. Wiley, New York.
10. Characklis, W. G. 1990. Biofilm Processes. pp. 195–231 In: W. G. Characklis and K. C. Marshall (eds.), Biofilms. Wiley, New York.
11. Christensen, F. R., Holm Kristensen, G., la Cour Jansen, J. 1989. Biofilm structure—an important and neglected parameter in waste water treatment. Water Sci. Technol. **21**: 805–814.
12. Doetsch, R. N., Cook, T. M. 1973. Introduction to bacteria and their ecology. University Park Press, Baltimore, MD.
13. Drury, W. J., Stewart, P. S., Characklis, W. G. 1993. Transport of 1-μm latex particles in *Pseudomonas aeruginosa* biofilms. Biotechnol. Bioeng. **42**: 111–117.
14. Gujer W., Wanner, O. 1990. Modelling mixed population biofilms. pp. 307–444 In: W. G. Characklis and K. C. Marshall (eds.), Biofilms. Wiley, New York.
15. Huang, C.-T., Peretti, S. W., Bryers, J. D. 1992. Use of flow cell reactors to quantify biofilm formation kinetics. Biotechnol. Techn. **6**: 193–198.
16. Korber, D. R., Lawrence, J. R., Sutton, B., Caldwell, D. E. 1989. Effect of laminar flow velocity on the kinetics of surface recolonization by Mot^+ and Mot^- *Pseudomonas fluorescens*. Microbiol. Ecol. **18**: 1–19.
17. Kornegay, B. H., Andrews, J. F. 1968. Kinetics of fixed-film biological reactors. J. Water Pollut. Control Fed. **40**: R460–R468.
18. Kugaprasatham, S., Nagaoka, H., Ohgaki, S. 1992. Effect of turbulence on nitrifying biofilms at non-limiting substrate conditions. Water Res. **26**: 1629–1638.
19. La Motta, E. J. 1976. Kinetics of growth and substrate uptake in a biological film system. Appl. Environ. Microbiol. **31**: 286–293.
20. Luria, S. E. 1960. The bacterial protoplasm: Composition and organization. pp. 1–34 In: I. C. Gunsalus and R. Y. Stanier (eds.), The bacteria, vol. I: Structure. Academic Press, New York.
21. Pedersen, K. 1990. Biofilm development on stainless steel and pvc surfaces in drinking water. Water Res. **24**: 239–243.
22. Quirynen, M., Marechal, M., van Steenberghe, D., Busscher, H. J., van der Mei, H. C. 1991. The bacterial colonization of intra-oral hard surfaces in vivo: Influence of surface free energy and surface roughness. Biofouling **4**: 187–198.
23. Rittmann, B. E., McCarty, P. L. 1980. Model of steady-state-biofilm kinetics. Biotechnol. Bioeng. **22**: 2343–2357.
24. Robinson, J. A., Trulear, M. G., Characklis, W. G. 1984. Cellular reproduction and extracellular polymer formation by *Pseudomonas aeruginosa* in continuous culture. Biotechnol. Bioeng. **26**: 1409–1417.
25. Santos, R., Callow, M. E., Bott, T. R. 1991. The structure of *Pseudomonas fluorescens* biofilms in contact with flowing systems. Biofouling **4**: 319–336.
26. Siebel, M. A., Characklis, W. G. 1991. Observations of binary population biofilms. Biotechnol. Bioeng. **37**: 778–789.
27. Siegrist, H., Gujer, W. 1985. Mass transfer mechanisms in a heterotrophic biofilm. Water Res. **19**: 1369–1378.
28. Stewart, P. S., Peyton, B. M., Drury, W. J., Murga, R. 1993. Quantitative observations of heterogeneities in *Pseudomonas aeruginosa* biofilms. Appl. Environ. Microbiol. **59**: 327–329.
29. Trulear, M. G., Characklis, W. G. 1982. Dynamics of biofilm processes. J. Water Pollut. Control Fed. **54**: 1288–1301.
30. Van de Graaf, A. A., de Bruijn, P., Robertson, L. A., Kuenen, J. G., Mulder, A. 1991. Biological oxidation of ammonium under anoxic conditions: Anammox process. pp. 667–670 In: H. Verachtert and W. Verstraete (eds.), Proceedings of the International Symposium on Environmental Biotechnology, vol. II. The Royal Flemish Society of Engineers, Antwerpen.
31. Van Schie, B. J., van Dijken, J. P., Kuenen, J. G. 1984. Non-coordinated synthesis of glucose dehydrogenase and its prosthetic group PQQ in *Acinetobacter* and *Pseudomonas* species. FEMS Microbiol. Lett. **24**: 133–138.
32. Verran, J., Lees, G., Shakespeare, A. P. 1991. The effect of surface roughness on the adhesion of *Candida albicans* to acrylic. Biofouling **3**: 183–192.
33. Wanner, O., Gujer, W. 1986. A multispecies biofilm model. Biotechnol. Bioeng. **28**: 314–328.